Mechanical Loading Overcomes High Interstitial Fluid Pressure in Metastatic Bone Tumors: A Computational Analysis

Rodrigo B. Guerra[1], Gene R. DiResta[2], Pat B. Zanzonico[3], John H. Healey[3], Susannah P. Fritton[1]
[1]City College of New York, New York, NY, [2]Microflow Associates, Pleasantville, NY, [3]Memorial Sloan Kettering Cancer Center, New York, NY
rguerra000@citymail.cuny.edu

Disclosures: Rodrigo B. Guerra (N), Gene R. DiResta (N), Pat B. Zanzonico (N), John H. Healey (N), Susannah P. Fritton (N)

Introduction: Cancer metastasis to bone can lead to a significantly reduced quality of life due to debilitating skeletal-related events. For the types of cancer that do not respond to hormone or antibody therapy, chemotherapy is a primary treatment option. The prognosis for these types of cancer can be improved by maximizing and retaining the chemo agent concentration at and around tumor areas, while keeping systemic concentration below toxic thresholds. Among the obstacles minimizing localized drug delivery is the presence of high interstitial fluid pressure within tumors, which is caused by irregular vascularity and absence of lymphatic drainage. It is known that loading-induced bone deformation enhances convective transport in bone tissue via interstitial fluid flow [1]. Our previous study showed that the uptake of ^{18}F-NaF was 47% higher in the tumor area after 10 minutes of mechanical loading of rat tumor-bearing tibias compared to no loading. We hypothesize that the increase in drug delivery is driven by changes in interstitial fluid movement within the bone and tumor, caused by bone deformation during loading. We test this hypothesis using finite element analysis of a multiphase poroelastic model of tumor-bearing tibias under compression.

Methods: PET/CT scans of tumor-bearing rat tibias (n=6) from our previous experiment were segmented using 3D Slicer (www.slicer.org) (**Fig. 1**). Characteristic dimensions of the tumor and the tibia were measured from the segmentations and then averaged (**Table 1**). 3D idealized geometries of the tumor and cortical bone were then constructed in ABAQUS (Dassault Systemes). The bone, marrow, and tumor geometries were assembled into two configurations: (1) the tumor interfacing only the marrow, (2) the tumor interfacing the marrow and cortical bone (**Fig. 1**). It was assumed that the dominant porosity of bone at the organ scale was that of the vascular porosity; elastic and permeability properties of cortical bone were thus based on this assumption (**Table 1**). Both idealized geometries were meshed using C3D10MP quadratic tetrahedral elements. Loading conditions were defined at the proximal surface of the models, while axial displacement was restricted at the distal surface (**Fig. 1**). The periosteal surface was considered impermeable, while free flow was assumed at the interface of materials. To model elevated tumor interstitial fluid pressure, a pore pressure of 40 mmHg was assigned at the tumor core (**Fig. 1**). Physiological loading that represented walking was applied to both models: 0.1% compression (1000 microstrain) at 1 Hz. An ABAQUS soils analysis was performed to calculate interstitial fluid velocities in the bone, marrow, and tumor.

Results: With no compression applied to the tibia, interstitial fluid flowed out of the tumor core due to the elevated tumor interstitial pressure (**Fig. 2**). Loading of the idealized tumor-bearing tibias overcame the high pressure at the tumor core and reversed the direction of interstitial fluid flow such that fluid flowed into the tumor during compression (**Fig. 2**). Location of the tumor within the bone affected the fluid distribution patterns within tumor tissue. In the case where tumor interfaced both marrow and cortical bone, fluid velocity magnitudes at the tumor/bone interface were one order of magnitude greater than the fluid velocity magnitudes at the tumor/marrow interface (**Fig. 2**).

Discussion: The results suggest that the pore pressure changes induced in bone and marrow by physiological mechanical loading of the tibia can overcome the high interstitial fluid pressures commonly found in cancerous bone tumors, thus directing the flow of interstitial fluid back into the tumor. While the analysis did not directly quantify solute/drug transport, the results support our previous experimental results that showed increased drug concentration in tumor tissues after mechanical loading. Current work is investigating rat-specific models and different loading conditions to further assess the mechanism by which mechanical interventions can influence interstitial fluid flow into bone tumors.

Significance: It is crucial to develop novel interventions to counteract drug resistance in tumors, as it remains a challenging obstacle in the improvement of cancer prognosis [2]. This computational analysis provides insight into the mechanisms behind improved drug delivery to tumors using bone loading and could aid in the development and optimization of individualized clinical protocols to improve treatment efficacy for metastatic cancer patients.

References: [1] Knothe Tate et al., J. Exp. Biol. 2000; [2] Nia et al., Clin. Cancer Res. 2019.
Acknowledgement: Supported by NIH grant U54CA132378.

Material Property	Cortical Bone	Marrow	Tumor
Young's Modulus, E (MPa)	1.7E+04	2.0E+00	4.5E-03
Permeability, k (mm^2)	6.30E-07	1.00E-11	5.90E-10
Porosity, ϕ	0.04	0.8	0.2
Characteristic Dimensions (n=6)			
Cortical Thickness (mm)	0.46 ± 0.03	-	-
Long Axis/Length (mm)	33.82 ± 0.82	-	3.37± 0.15
Short Axis/Radius (mm)	1.56 ± 0.11	-	1.68 ± 0.05
Distance from Growth Plate (mm)	-	-	3.24 ± 0.88

Table 1. Summary of the poroelastic material properties used in the models, and summary of cortical bone and tumor dimensions measured from rat PET/CT scans (n=6).

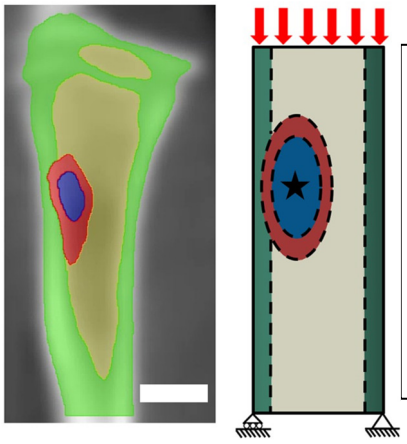

Figure 1. Left: Lateral cut of the segmentation from a PET/CT scan of a tumor-bearing rat tibia radiolabeled with ^{18}F-FDG. Scale bar: 2 mm.
Right: Idealized model with tumor interfacing both marrow and cortical bone. Compression was applied axially (arrows) at the proximal surface and fixed axially at the distal surface. A pore pressure of 40 mmHg was assigned to the tumor core (marked with ★).

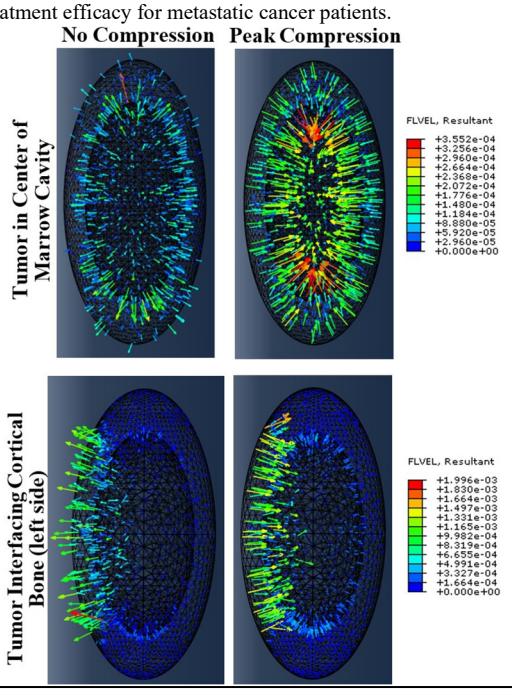

Figure 2. Distribution of interstitial fluid velocity resultant vectors (FLVEL, mm/s) within the tumor tissue before and after applying 0.1% peak compression at 1 Hz for both idealized model configurations. The direction of the velocity vectors during peak loading is reversed.